

# Siloxanol-Functionalized Copper Iodide Cluster as a Thermo-chromic Luminescent Building Block

Sandrine Perruchas,<sup>\*,†</sup> Nicolas Desboeufs,<sup>†</sup> Sébastien Maron,<sup>†</sup> Xavier F. Le Goff,<sup>‡</sup> Alexandre Fargues,<sup>§</sup> Alain Garcia,<sup>§</sup> Thierry Gacoin,<sup>†</sup> and Jean-Pierre Boilot<sup>\*,†</sup>

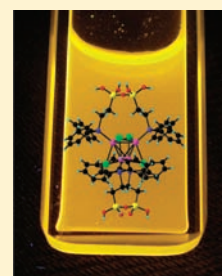
<sup>†</sup>Laboratoire de Physique de la Matière Condensée (PMC), CNRS, Ecole Polytechnique, 91128 Palaiseau Cedex, France

<sup>‡</sup>Laboratoire Hétéroéléments et Coordination (DCPH), CNRS, Ecole Polytechnique, 91128 Palaiseau Cedex, France

<sup>§</sup>Institut de Chimie de la Matière Condensée de Bordeaux (ICMCB), CNRS, 87 Avenue du Dr A. Schweitzer, 33608 Pessac Cedex, France

## Supporting Information

**ABSTRACT:** A copper iodide cluster bearing reactive silanol groups exhibits thermo-chromic luminescence properties sensitive to its chemical environment and is thus a suitable building block for the synthesis of optically active materials.



## INTRODUCTION

Photoluminescent materials are currently an active domain of research driven by their broad range of applications in light-emitting devices.<sup>1</sup> In this prospect, transition-metal coordination compounds have attracted considerable interest because of their various photophysical properties.<sup>2,3</sup> Among them, first-row transition-metal compounds are attractive from an economical point of view, while they are less toxic and more easily available than the noble-metal complexes. The molecular tetracopper(I) iodide clusters formulated as  $[\text{Cu}_4\text{I}_4\text{L}_4]$  (L = organic ligand)<sup>4–6</sup> are particularly appealing because of their rich photoluminescence properties,<sup>5,7,8</sup> which can be exploited to access materials exhibiting original optical properties.<sup>9,10</sup> In this context, the sol–gel process presents several advantages to design materials for optical applications because of its chemical and processing versatility.<sup>11</sup> Numerous silica- and/or siloxane-based hybrid organic–inorganic emissive materials have thus been developed.<sup>12</sup> Compounds containing silanol groups (SiOH) represent an interesting class of precursors for these kinds of materials.<sup>13</sup> Indeed, upon condensation reaction, strong siloxane (Si–O–Si) bonds are formed, which can lead to polysiloxane polymeric derivatives, supramolecular organo-silicon compounds, as well as discrete assemblies like metallasiloxanes.<sup>14–16</sup> While characterization of the precursors is essential to the comprehension of the properties exhibited by the final material, isolation of these functionalized compounds, prior to their polymerization, is often difficult mainly because of the high reactivity of the silanols toward condensation.

Here, we report on the synthesis and structural and optical characterization of a siloxanol-functionalized luminescent cluster, namely,  $[\text{Cu}_4\text{I}_4(\text{PPh}_2(\text{CH}_2)_2\text{Si}(\text{OH})_2\text{OSi}$

$(\text{OH})_2(\text{CH}_2)_2\text{PPh}_2)_2]$  (**2**), obtained through hydrolysis and condensation reactions of the corresponding alkoxy-silane cluster  $[\text{Cu}_4\text{I}_4(\text{PPh}_2(\text{CH}_2)_2\text{Si}(\text{OEt})_3)_4]$  (**1**). In this original disiloxane cluster (**2**), the ligands exhibit intracuster condensation, but silanol groups are also formed and isolated without intercluster condensation. Temperature-dependent luminescence measurements of **2** revealed emissions sensitive to the chemical environment. Constraints in the solid state due to an efficient hydrogen-bonding network involving the silanol groups are probably responsible for this phenomenon. Finally, the reactivity of this siloxanol cluster toward further condensation reaction with the usual sol–gel precursors is demonstrated, making this cluster an unprecedented building block for the synthesis of thermo-chromic luminescent materials.

## EXPERIMENTAL SECTION

All manipulations were performed with standard air-free techniques using Schlenk equipment, unless otherwise noted. Solvents were distilled from the appropriate drying agents and degassed prior to use. Copper(I) iodide and tetramethoxysilane (TMOS) were purchased from Aldrich and used as received. Diphenylethyltriethoxysilane-phosphine  $[\text{PPh}_2(\text{CH}_2)_2\text{Si}(\text{OCH}_2\text{CH}_3)_3]$  was synthesized by the method reported in the literature.<sup>17</sup>

**Synthesis of 2.** To a suspension of CuI (0.6 g, 3.1 mmol) in dichloromethane (20 mL) was added the phosphine ligand  $\text{PPh}_2(\text{CH}_2)_2\text{Si}(\text{OCH}_2\text{CH}_3)_3$  (1.05 g, 2.8 mmol). The solution was stirred for 12 h at room temperature. The mixture was filtered, and after evaporation of the solvent, the product was recovered as a colorless oil. The latter was dissolved in tetrahydrofuran (THF; 12

Received: April 1, 2011

Published: December 23, 2011

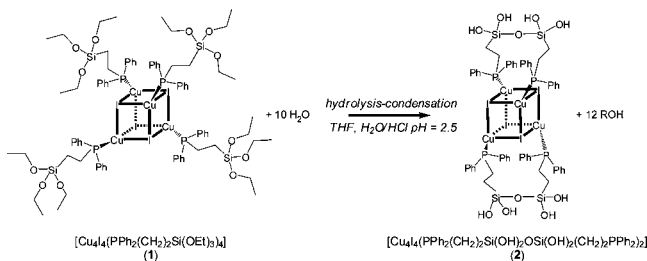
mL), and H<sub>2</sub>O–HCl (pH 2.5, 1 mL) was added. The clear solution was left to stand at room temperature, and after 2 days, colorless crystals of the formula [Cu<sub>4</sub>I<sub>4</sub>(PPh<sub>2</sub>(CH<sub>2</sub>)<sub>2</sub>Si(OH)<sub>2</sub>OSi(OH)<sub>2</sub>(CH<sub>2</sub>)<sub>2</sub>PPh<sub>2</sub>)<sub>2</sub>·4THF] were obtained. Yield: 66% (1 g, 0.46 mmol). Liquid-state NMR: <sup>1</sup>H (300.06 MHz, DMF) δ 0.98–1.03 (2 H, m, CH<sub>2</sub>CH<sub>2</sub>Si), 2.52–2.55 (2 H, m, PCH<sub>2</sub>CH<sub>2</sub>), 6.48 (2 H, s, SiOH), 7.44–7.52 (6 H, m, Ph), 7.82–7.78 (4 H, m, Ph); <sup>31</sup>P (145.77 MHz, DMF) δ –24.8 (br); <sup>29</sup>Si (71.54 MHz, DMF) δ –51.8 (d). Solid-state MAS (magic angle spinning) NMR: <sup>31</sup>P: δ –26.3 (q); <sup>29</sup>Si: δ –50.6 (d). EDX anal. Calcd (atom %) for Cu<sub>4</sub>I<sub>4</sub>P<sub>4</sub>Si<sub>4</sub>: Cu, 25; I, 25; P, 25; Si, 25. Found: Cu, 24.3 (0.6); I, 26.8 (0.2); P, 22.0 (0.2); Si, 26.9 (0.6). Anal. Calcd (wt %) for C<sub>56</sub>H<sub>64</sub>O<sub>10</sub>Si<sub>4</sub>P<sub>4</sub>Cu<sub>4</sub>I<sub>4</sub> + 4C<sub>4</sub>H<sub>8</sub>O: C, 39.60; H, 4.43. Found: C, 39.40; H, 4.58.

**Synthesis of 3.** To TMOS (2.2 mL, *n*<sub>Si</sub> = 15 mmol) was added cluster 2 (400 mg, 1.8 × 10<sup>−4</sup> mol, *n*<sub>Si</sub> = 1.5 mmol). The white suspension was left to stir for 2 days at room temperature until the solution became clear. A white precipitate was obtained by the addition of EtOH to the solution. After filtration, the solid was washed with EtOH and dried under a vacuum (*m* = 440 mg). Several experiments gave reproducible results. Liquid-state NMR: <sup>1</sup>H (300.06 MHz, CDCl<sub>3</sub>) δ 0.77–1.26 (2 H, m, CH<sub>2</sub>CH<sub>2</sub>Si), 2.14–2.54 (2 H, m, PCH<sub>2</sub>CH<sub>2</sub>), 3.46 (10 H, m, CH<sub>3</sub>), 7.00–7.78 (10 H, m, Ph); <sup>31</sup>P (145.77 MHz) δ –24.9 (br). Solid-state MAS NMR: <sup>31</sup>P δ –21.5 (br); <sup>29</sup>Si δ –58.2 (br, T<sup>2</sup> Si<sub>cluster</sub>), –67.7 (br, T<sup>3</sup> Si<sub>cluster</sub>), –86.0 (br, Q<sup>1</sup> TMOS), –93.9 (br, Q<sup>2</sup> TMOS). EDX anal. Calcd (atom %) for Cu<sub>4</sub>I<sub>4</sub>P<sub>4</sub>Si<sub>10</sub>: Cu, 18.2; I, 18.2; P, 18.2; Si, 45.4. Found: Cu, 19.1 (0.7); I, 19.4 (0.5); P, 15.7 (0.3); Si, 45.8 (0.9). Anal. Calcd (wt %) for C<sub>56</sub>H<sub>59</sub>O<sub>10</sub>Si<sub>4</sub>P<sub>4</sub>Cu<sub>4</sub>I<sub>4</sub> + 5Si(OCH<sub>3</sub>)<sub>3</sub> + 10Si(OCH<sub>3</sub>)<sub>2</sub>: C, 33.69; H, 4.26. Found: C, 33.89; H, 4.20.

## RESULTS AND DISCUSSION

Cluster 2 is synthesized in solution starting from compound 1 (see the Experimental Section). The latter was previously obtained from the reaction of CuI with the alkoxy silane phosphine ligand PPh<sub>2</sub>(CH<sub>2</sub>)<sub>2</sub>Si(OCH<sub>2</sub>CH<sub>3</sub>)<sub>3</sub>. As we have reported, 1 is recovered as oil due to uncontrolled partial hydrolysis and condensation of the ligand by air exposure, thus preventing structural characterization.<sup>10</sup> In order to induce on purpose hydrolysis and condensation of the alkoxy silane groups, 1 was reacted in an acidic medium (THF/H<sub>2</sub>O–HCl, pH 2.5), leading to cluster 2 as a crystalline powder in high yield (66%), as illustrated in Scheme 1.

### Scheme 1. Cluster 2 Synthesis



From single-crystal X-ray diffraction analysis (see the Supporting Information, SI), 2 crystallizes in the tetragonal space group *I*4<sub>1</sub>/*a*, with the molecular structure depicted in Figure 1. This cluster presents a [Cu<sub>4</sub>I<sub>4</sub>] cubane structure formed by four copper atoms and four iodine atoms, which occupy alternatively the corners of a distorted cube. The phosphine ligands are coordinated to each copper atom by the phosphorus atom, and the hydrolysis and condensation reactions of two alkoxy silane Si(OEt)<sub>3</sub> groups result in the formation of two intracluster siloxane Si–O–Si bonds.

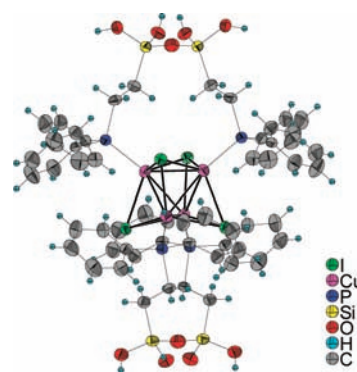


**Figure 1.** Molecular structure of 2 in a thermal ellipsoid plot (probability factor 50%).

Among the 12 initial alkoxy silane SiOCH<sub>2</sub>CH<sub>3</sub> functions, 4 have been condensed into Si–O–Si bonds and 8 have been hydrolyzed into SiOH groups. The cluster is thus formulated as [Cu<sub>4</sub>I<sub>4</sub>(PPh<sub>2</sub>(CH<sub>2</sub>)<sub>2</sub>Si(OH)<sub>2</sub>OSi(CH<sub>2</sub>)<sub>2</sub>(OH)<sub>2</sub>PPh<sub>2</sub>)<sub>2</sub>] (2) with the ligands now chelating. Elemental analyses and Fourier transform infrared (FTIR) and NMR characterizations confirm this formula (see the SI). The silanol protons are revealed in the liquid-state <sup>1</sup>H NMR spectra as a singlet at 6.48 ppm. As expected, in the FTIR spectrum, the Si–OH stretching band is observed at 825 cm<sup>−1</sup> and the O–H ones appear as a broader peak centered at 3400 cm<sup>−1</sup>. Concerning the Si–O–Si bonds, the Si–O antisymmetric stretching vibrations correspond to a broad band centered at 1100 cm<sup>−1</sup>.

The ligands present a chelating geometry relatively rare for these cubane copper iodide clusters. The only other example reported with the bis(ethylamidophosphine) ligand leads to a relatively distorted [Cu<sub>4</sub>I<sub>4</sub>] cluster core.<sup>18</sup> The Cu–I [2.736(1), 2.665(1), and 2.675(1) Å] and Cu–P [2.240(1) Å] bond distances in cluster 2 are within the range of reported values for copper iodide clusters coordinated with diphenylphosphine derivatives. The siloxane bond presents an expected value for the Si–O distance of 1.609(1) Å, but the Si–O–Si angle is more unusual, with a high value of 175.5(3)°. The almost linearity of the Si–O–Si angle has also been reported for [t-BuSi(OH)<sub>2</sub>]<sub>2</sub>O and has been attributed to the absence of intramolecular hydrogen bonding involving the silanol groups.<sup>19</sup> The Cu–Cu distances [2.704(1) and 2.743(1) Å] are the shortest reported in the literature for similar clusters with phosphine ligands, which generally lie in the range 2.8–3.1 Å.<sup>20</sup> These distances are even comparable to those reported for pyridine derivatives, although previous studies showed that Cu–Cu bonds in [Cu<sub>4</sub>I<sub>4</sub>L<sub>4</sub>] clusters based on phosphine ligands are generally significantly longer.<sup>21</sup> This is probably due to the steric constraints induced by condensation of the ligands. This “chelating effect” is less significant for the larger bis(ethylamidophosphine) ligand, which induces less constraints.<sup>18</sup> These Cu–Cu values, shorter than the sum of the van der Waals radii of copper(I) (2.80 Å),<sup>22</sup> imply strong metal–metal bonding interactions in cluster 2. This is an important point because Cu–Cu interactions have been reported to greatly influence the luminescence properties of the copper iodide clusters.<sup>5</sup>

The crystal structure of 2 can be described as an assembly of chains of clusters running along the *c* axis (see Figure 2 and the unit cell content in Figure S2 in the SI). THF solvent molecules are incorporated within the structure and are located between the cluster chains. In these chains, adjacent clusters are linked

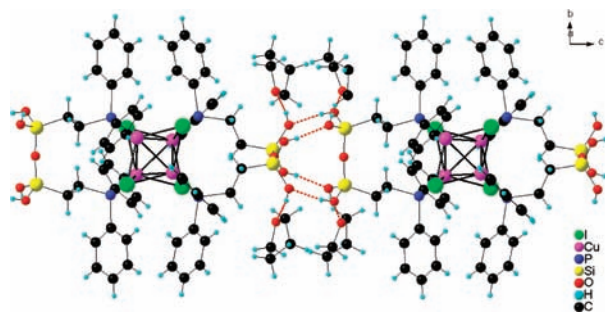


Figure 2. Hydrogen-bonding network in the crystal structure of **2**.

by hydrogen bonds between the SiOH groups ( $\text{SiOH}\cdots\text{OSi} = 2.009 \text{ \AA}$ ). The hydrogen-bonding network is shown in Figure 2 and corresponds to the  $R_2^2(10)$  motif in the Etter coding.<sup>23</sup> One of the two SiOH groups is also involved in hydrogen bonding, with the oxygen atoms of the THF molecules acting as hydrogen-bond acceptors ( $\text{SiOH}\cdots\text{O}_{\text{THF}} = 1.858 \text{ \AA}$ ). FTIR analyses confirm this hydrogen-bonding network involving all of the silanol groups by the large peak observed at  $3400 \text{ cm}^{-1}$ . Although here the SiOH groups are in close contact ( $\text{SiO}\cdots\text{OSi} = 2.731 \text{ \AA}$ ), they are not condensed into a Si–O–Si bond because of steric hindrance. Indeed, the condensation of the eight SiOH groups two by two would result in too high constraint in the tetrahedral geometry of the silicon atom.

At room temperature, **2** is a white powder under ambient light (Figure 3a), which under UV excitation emits an intense

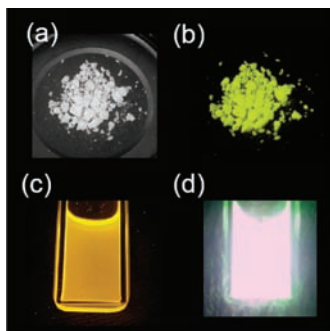


Figure 3. Photographs of **2**: in powder at room temperature (a) under ambient light and (b) under UV irradiation at 312 nm (UV lamp) and dissolved in DMF (c) at room temperature and (d) in liquid nitrogen at 77 K.

yellow light in powder and in solution (Figures 3b,c). The thermochromic luminescence properties are revealed by dipping the samples into liquid nitrogen. The yellow emission of the cluster in solution turns bright purple (Figure 3d) and is progressively recovered upon warming to room temperature, indicating a completely reversible thermochromic luminescence. This is different for these clusters in the solid state whose the emission color does not change by lowering of the temperature.

Emission and excitation spectra recorded for **2** in the solid state and in solution from 290 K down to 20 K are shown in Figure 4. At 290 K, the emission spectra display a single broad emission band centered at 570 nm for the cluster in powder and at 595 nm in solution ( $\lambda_{\text{ex}} = 300 \text{ nm}$ ). This is in agreement with the yellow light observed at room temperature, which can be attributed to the “cluster-centered” (CC) emission band characteristic of these clusters.<sup>24</sup> The 25 nm shift observed is

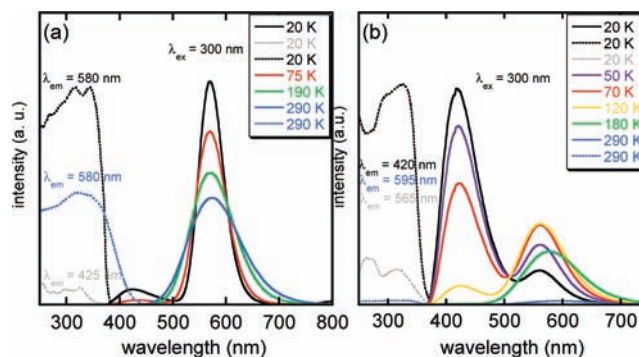


Figure 4. Temperature-dependent luminescence spectra of **2** from 20 to 290 K (a) in the solid state and (b) in a DMF solution. Emission ( $\lambda_{\text{ex}} = 300 \text{ nm}$ ) and excitation spectra are solid and dotted lines, respectively.

due to weaker rigidity in solution compared to the solid state, as was already observed for similar clusters. This phenomenon, named the “rigidochromic effect”, has been attributed to the effect of medium rigidity due to distortion of the  $^3\text{CC}$  state relative to the ground state.<sup>5</sup> The internal luminescence quantum yield of the cluster was measured at 290 K in the solid state, and a high value of 60% was obtained for  $\lambda_{\text{ex}} = 360 \text{ nm}$ . By lowering of the temperature of the cluster in powder, down to 20 K, the intensity of the CC band progressively increased along with the narrowing of the bandwidth (Figure 4a). No shift of the band was observed. Around 80 K, a new emission band of low intensity appeared at higher energy,  $\lambda_{\text{max}} = 420 \text{ nm}$ , corresponding to the halide-to-ligand charge-transfer (XLCT) transition classically observed for these clusters at low temperature.<sup>24</sup> For the cluster in solution, by lowering of the temperature, the intensity of the CC emission progressively increased to 80 K (Figure 4b). A blue shift of the band was observed with  $\lambda_{\text{max}} = 595 \text{ nm}$  at 290 K and  $\lambda_{\text{max}} = 560 \text{ nm}$  below 150 K. This phenomenon is due to solidification of the solvent after the glass transition ( $T_{\text{DMF}} = 212 \text{ K}$ ) and is also attributed to the “rigidochromic effect” previously mentioned. At 180 K, the XLCT emission band appeared at  $\lambda_{\text{max}} = 420 \text{ nm}$ , and below 80 K, its intensity progressively increased with the concomitant decrease of the CC band. At 80 K, the intensities of the two emission bands were similar, giving the purple emission observed in liquid nitrogen by the addition of the yellow and blue lights (Figure 3d). At 20 K, the XLCT band was largely predominant, opposite to the cluster in the solid state.

Cluster **2** in solution thus exhibits the thermochromic luminescence classically observed for  $[\text{Cu}_4\text{I}_4\text{L}_4]$  clusters with the two emission bands CC and XLCT, whose relative intensities vary in temperature.<sup>5</sup> This contrasts with the luminescent behavior of the cluster in crystalline powder because the appearance of the XLCT emission band seems to be prevented. The communication between the two emission states, whose populations are normally in thermal equilibrium, seems to be perturbed in the solid state. This particular emissive behavior could originate from the cluster assembly, which induces “constraints” in the solid state, thus preventing the communication between the two excited states. This can be related to the efficient hydrogen-bonding network observed between the clusters in the crystal structure, but the exact effect responsible for the XLCT band quenching is difficult to evaluate at this stage. Another unexpected emissive behavior is



the absence of CC band shift upon lowering of the temperature both in the solid state and in solution. This is surprising because such cubane clusters usually present a red shift due to shortening of the Cu–Cu bond at low temperature.<sup>25</sup> This phenomenon can be attributed to the chelating character of the ligand, which limits the flexibility of the cluster, thus preventing Cu–Cu bond variation.

Finally, cluster **2** was reacted with an alkoxysilane derivative in order to demonstrate the reactivity of the silanol groups toward further condensation. Upon reaction with TMOS, a white solid (**3**) was precipitated and characterized (NMR, FTIR, EDX, and elemental analysis in the Experimental Section and SI). The appearance of new peaks ( $T^2$ ,  $T^3$ ,  $Q^1$ , and  $Q^2$ ) in the solid-state  $^{29}\text{Si}$  NMR spectra<sup>26</sup> along with  $^{31}\text{P}$  signals identical with those of **2**, is consistent with the reaction of the silicon atoms without cluster alteration (spectra in the SI). These new  $^{29}\text{Si}$  peaks correspond to the condensation product of one ( $T^2$ ) and two ( $T^3$ ) TMOS molecules per  $\text{Si}(\text{OH})_2$  group (details in the SI).<sup>27</sup> This leads to a mixture of condensation products for **3** with six TMOS molecules on average per cluster. These results confirm the covalent attachment of the alkoxysilane derivative to the cluster via the Si–O–Si bond and thus the reactivity of the SiOH groups.

The photoluminescent properties of **3** were investigated. The internal luminescence quantum yield measured at 290 K is 17% ( $\lambda_{\text{ex}} = 340 \text{ nm}$ ). The temperature-dependent luminescence spectra recorded for **3** are shown in Figure 5a. A behavior quite

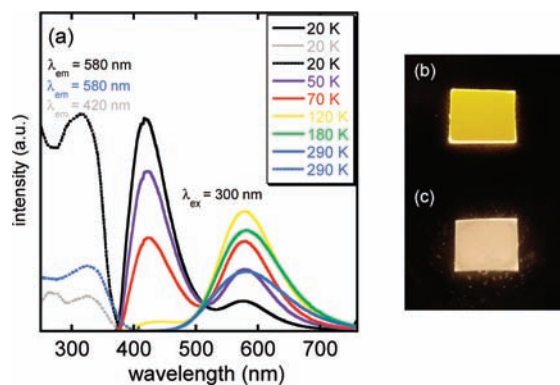


**Figure 5.** (a) Temperature-dependent luminescence spectra of **3** from 20 to 290 K in the solid state. Emission ( $\lambda_{\text{ex}} = 300 \text{ nm}$ ) and excitation spectra are solid and dotted lines, respectively. Sol-gel thin film of **3** on a glass substrate ( $1 \times 1 \text{ cm}^2$ ) under UV irradiation at 312 nm (b) at 298 K and (c) at 77 K.

similar to that of cluster **2** in solution is observed, with the intensities of the two emission bands (XLCT and CC) varying in temperature, which is characteristic of thermochromic luminescence properties. As expected, there is no blue shift of the CC band because no “rigidochromic effect”, due to solvent solidification, occurs in this case. Note also that the intensity of the CC band at room temperature (290 K) is not negligible compared to the one for the cluster in solution. This effect can be attributed to less nonradiative phenomenon induced by the solvent. In opposition with the cluster in the solid state, no quenching of the XLCT band is observed, which is consistent with different intercluster interactions in **3** (different hydrogen-bonding network). Compound **3** can also be processed into film. As shown in Figure 5b,c, by spin coating of the liquid obtained from the reaction of **2** with TMOS on a

glass substrate, a transparent and emissive “sol-gel” thin film can be obtained with the thermochromic luminescence properties of **3** preserved (corresponding spectra reported in Figure S4 in the SI).

## CONCLUSION

In conclusion, this siloxanol cluster, perfectly characterized, is a neat building block for the synthesis of “sol-gel” materials. The presence of eight SiOH groups per molecular unit assures the reactivity of the cluster toward further condensation reactions and thus the grafting of molecules of potential interest. This highly luminescent cluster whose emission properties vary with the temperature and chemical surroundings has thus great potential for the synthesis of light-emitting materials, in sensor applications for instance. In this prospect, the preparation of functional luminescent materials using this cluster as an emissive building block is currently in progress.

## ASSOCIATED CONTENT

### Supporting Information

Characterization details and X-ray crystallographic data in CIF format. This material is available free of charge via the Internet at <http://pubs.acs.org>.

## AUTHOR INFORMATION

### Corresponding Author

\*E-mail: [sandrine.perruchas@polytechnique.edu](mailto:sandrine.perruchas@polytechnique.edu). Phone: (+33) (0)1 69 33 46 85. Fax: (+33) (0)1 69 33 47 99.

## ACKNOWLEDGMENTS

The authors thank the CNRS for funding.

## REFERENCES

- Jüstel, T.; Nikol, H.; Ronda, C. *Angew. Chem., Int. Ed.* **1998**, *37*, 3084–3103.
- Ulbricht, C.; Beyer, B.; Friebe, C.; Winter, A.; Schubert, U. S. *Adv. Mater.* **2009**, *21*, 4418–4441.
- Fernandez-Moreira, V.; Thorp-Greenwood, F. L.; Coogan, M. P. *Chem. Commun.* **2010**, *46*, 186–202.
- Barbieri, A.; Accorsi, G.; Armaroli, N. *Chem. Commun.* **2008**, 2185–2193.
- Ford, P. C.; Cariati, E.; Bourassa, J. *Chem. Rev.* **1999**, *99*, 3625–3647.
- Yam, V. W.-W.; Lo, K. K.-W. *Chem. Soc. Rev.* **1999**, *28*, 323–334.
- Radjaipour, M.; Oelkrug, D. *Ber. Bunsen-Ges. Phys. Chem.* **1978**, *82*, 159–163.
- Perruchas, S.; Le Goff, X. F.; Maron, S.; Maurin, I.; Guillen, F.; Garcia, A.; Gacoïn, T.; Boilot, J.-P. *J. Am. Chem. Soc.* **2010**, *132*, 10967–10969.
- Braga, D.; Maini, L.; Mazzeo, P. P.; Ventura, B. *Chem.—Eur. J.* **2010**, *16*, 1553–1559.
- Tard, C.; Perruchas, S.; Maron, S.; Le Goff, X. F.; Guillen, F.; Garcia, A.; Vigneron, J.; Etcheberry, A.; Gacoïn, T.; Boilot, J.-P. *Chem. Mater.* **2008**, *20*, 7010–7016.
- Brinker, C. J.; Scherrer, G. W. *Sol-Gel Science, The Physics and Chemistry of Sol-Gel Processing*; Academic Press: San Diego, CA, 1990.
- Sanchez, C.; Lebeau, B.; Chaput, F.; Boilot, J.-P. *Adv. Mater.* **2003**, *15*, 1969–1994 and references cited therein.
- Lickiss, P. D. *Adv. Inorg. Chem.* **1995**, *42*, 147–252.
- Kurashina, T.; Aoki, S.; Hirasawa, R.; Hasegawa, T.; Kasahara, Y.; Yoshida, S.; Yoza, K.; Nomiya, K. *Dalton Trans.* **2009**, 5542–5550.
- (a) Murugavel, R.; Chandrasekhar, V.; Roesky, H. W. *Acc. Chem. Res.* **1996**, *29*, 183–189. (b) Murugavel, R.; Voigt, A.; Walawalkar, M. G.; Roesky, H. W. *Chem. Rev.* **1996**, *96*, 2205–2236.

- (16) MacLachlan, M. J.; Zheng, J.; Lough, A. J.; Manners, I. *Organometallics* **1999**, *18*, 1337–1345.
- (17) Bunlaksanusorn, T.; Knochel, P. *Tetrahedron Lett.* **2002**, *43*, 5817–5820.
- (18) Li, Y.; Yung, K.-F.; Chan, H.-S.; Wong, W.-T. *Inorg. Chem. Commun.* **2003**, *6*, 1451–1453.
- (19) (a) Seto, I.; Gunji, T.; Kumagai, K.; Arimitsu, K.; Abe, Y. *Bull. Chem. Soc. Jpn.* **2003**, *76*, 1983–1987. (b) O’Leary, B.; Spalding, T. R.; Ferguson, G.; Glidewell, C. *Acta Crystallogr.* **2000**, *B56*, 273–286.
- (20) Cambridge Structural Data Base. CCDC version 5.31.
- (21) Vega, A.; Saillard, J.-Y. *Inorg. Chem.* **2004**, *43*, 4012–1018.
- (22) Bondi, A. J. *Phys. Chem.* **1964**, *68*, 441–451.
- (23) Etter, M. C. *Acc. Chem. Res.* **1990**, *23*, 120–126.
- (24) De Angelis, F.; Fantacci, S.; Sgamellotti, A.; Cariati, E.; Ugo, R.; Ford, P. C. *Inorg. Chem.* **2006**, *45*, 10576–10584.
- (25) Kim, T. H.; Shin, Y. W.; Jung, J. H.; Kim, J. S.; Kim, J. *Angew. Chem., Int. Ed.* **2008**, *47*, 685–688.
- (26) Devreux, F.; Boilot, J. P.; Chaput, F.; Lecomte, A. *Phys. Rev. A* **1990**, *41*, 6901–6909.
- (27) Note that these signals cannot be attributed to pure cluster condensation products because the cluster does not react on itself; several attempts for this purpose were all unsuccessful.